

# Dynamic echo planar MR imaging of lung ventilation with hyperpolarized $^3\text{He}$ in normal subjects and patients with severe emphysema

David S. Gierada,<sup>1\*</sup> Brian Saam,<sup>2</sup> Dmitriy Yablonskiy,<sup>1</sup> Joel D. Cooper,<sup>3</sup> Stephen S. Lefrak<sup>3</sup> and Mark S. Conradi<sup>2</sup>

<sup>1</sup>Mallinckrodt Institute of Radiology, St Louis, MO 63110, USA

<sup>2</sup>Washington University, Physics-1105, St Louis, MO 63130, USA

<sup>3</sup>Barnes-Jewish Hospital, St Louis, MO 63110, USA

Received 13 October 1999; revised 20 December 1999; accepted 23 December 1999

**ABSTRACT:** We applied the rapid imaging capability of echo planar MR pulse sequences and hyperpolarized  $^3\text{He}$  ventilation imaging to observe the dynamic distribution of gas in the lungs during breathing. Findings in five normal volunteers (age 19–53 years) and four patients with severe smoking-related emphysema (age 56–71 years) were compared. All studies were performed on a 1.5 T whole body scanner using a 30 cm Helmholtz surface coil and 0.5 l of 20–40% polarized  $^3\text{He}$  mixed with 1–2 l nitrogen. Our echo planar imaging pulse sequence allowed acquisition of each image in 0.04 s, with a pixel size of  $7\text{ mm}^2$  ( $TR = 40.5\text{ ms}$ ,  $TE = 12.1\text{ ms}$ , flip angle =  $22^\circ$ , echo train length = 32, matrix =  $32 \times 64$ , field of view =  $225 \times 450\text{ mm}$ , slice thickness = 10 mm). Imaging was performed in the transaxial plane repeatedly at 3, 10 or 20 evenly spaced levels, immediately before and during breathing of the gas mixture. In normal subjects during the first breath,  $^3\text{He}$  appeared throughout each slice first in the mid lungs, then in the lower lungs, then in the upper lungs, with slightly greater signal in the dependent posterior regions. In patients with emphysema, sequential filling of different lung regions was seen during the first breath, with delayed filling of other regions observed during rebreathing and room air washout. We conclude that subsecond dynamic  $^3\text{He}$  MR ventilation imaging can reveal normal and abnormal ventilation phenomena not seen with conventional scintigraphic methods, and offers another approach to the study of ventilation physiology and pathophysiology. Copyright © 2000 John Wiley & Sons, Ltd.

**KEYWORDS:** MRI; hyperpolarized gases; EPI; dynamic imaging; lung ventilation; emphysema

## INTRODUCTION

Over the past few decades, ventilation imaging has been performed with radioactive gases or radiolabeled aerosol scintigraphy. Scintigraphy using radioactive gases allows assessment of ventilation on time scales of seconds to minutes, with the typical image acquisition time of 15 s. Radiolabeled aerosol scintigraphy allows static tomographic imaging of the lungs with single photon emission computed tomography (SPECT), but does not provide dynamic information about gas flow, and is of limited value in patients with chronic obstructive pulmonary disease, due to deposition of aerosolized particles in the central airways.

More recently, imaging of ventilation by MR imaging of hyperpolarized gases has become feasible.<sup>1–4</sup> Com-

pared to scintigraphy, this method can provide greater spatial resolution and more detailed depiction of the regional distribution of gas in the lungs, since tomographic sections, rather than projection images, are acquired. There have now been multiple reports of anatomic imaging of the lung airspaces with static breath-hold technique following inhalation of a bolus of hyperpolarized gas, in normal subjects and patients with pulmonary diseases.<sup>1–7</sup> An additional difference of MR that can be exploited in ventilation imaging is greater temporal resolution, using pulse sequences that acquire repeated images in less than 1 s. Echo planar imaging (EPI) techniques allow numerous excitations with less consumption of the nonrenewable gas hyperpolarization, compared to FLASH imaging, provided the voxel size is not too small (i.e.  $\geq 5\text{ mm}$ ).<sup>8</sup> It is thus now possible to study the time-dependent distribution of gas within the lungs during a single inspiration, without exposure to ionizing radiation, and with greater spatial resolution and signal-to-noise than with scintigraphic methods. In this report, we describe the dynamic regional distribution of  $^3\text{He}$  in the lungs as observed with subsecond dynamic

\*Correspondence to: D. S. Gierada, Mallinckrodt Institute of Radiology 216 S Kingshighway Blvd, St Louis, MO 63110, USA; e-mail: gieradad@mir.wustl.edu  
Contract/grant sponsor: Whitaker Foundation.

**Abbreviations used:** EPI, echo planar imaging; SPECT, single photon emission computed tomography.

EPI, comparing normal subjects and patients with severe emphysema.

## EXPERIMENTAL

For normal subjects we chose five volunteers without a history of cigarette smoking, and with no known acute or chronic pulmonary disease. There were two women, aged 19 and 24 years, and three men, aged 23, 27 and 53 years. Our four subjects with severe emphysema were patients selected for bilateral lung volume reduction surgery. There were three women, aged 56, 67 and 71 years, and one man, aged 63 years. All patients had severe obstructive pulmonary disease, with residual volumes greater than 300% of predicted and forced expiratory volume in 1 s ranging from 17 to 28% of predicted. All had evidence of severe emphysema on X-ray computed tomography.

Imaging studies were performed on a 1.5 T whole body scanner (Vision, Siemens Medical Systems, Erlangen, Germany) using a 30 cm Helmholtz coil built by two of the authors and adaptable to both the  $^3\text{He}$  frequency of 48.47 MHz and the  $^1\text{H}$  frequency of 63.63 MHz. For anatomic localization,  $^1\text{H}$  images were acquired in the transaxial plane, from the lung apices through the lung bases. A two-dimensional FLASH pulse sequence was used, with  $TR = 11$  ms,  $TE = 4.2$  ms,  $18^\circ$  flip angle, 10 mm section thickness,  $128 \times 128$  matrix, and 45 cm field of view. Images were acquired during natural quiet breathing.

For  $^3\text{He}$  ventilation studies, we performed transaxial imaging using a coarse grid EPI pulse sequence with a constant phase encoding gradient, a sinusoidal readout gradient with an oscillating period of 1.2 ms and amplitude of 11.5 mT/m,  $TR = 40.5$  ms,  $TE = 12.1$  ms,  $22^\circ$  flip angle, echo train length = 32, 10 mm section thickness,  $32 \times 64$  matrix, and  $225 \times 450$  mm field of view, producing a pixel size of  $7 \text{ mm}^2$ . The flip angle was calibrated on a  $^3\text{He}$  Boltzmann-polarized phantom. The signal amplitude vs pulse amplitude was fitted to the expected sinusoidal dependence. Each excitation covered an entire section, thus total time per image was the same as  $TR$  (0.04 s). The lungs were scanned sequentially and repeatedly in a cephalocaudal direction at 3, 10 or 20 evenly spaced levels, resulting in image acquisition intervals of 0.12, 0.40 or 0.80 s, respectively, at each individual scanned level.

The  $^3\text{He}$  gas (Spectra Gases, Irvington, NJ) was purified using an UltraPure PF Series Mini PF filter (NuPure, Manotick, Ontario, Canada). Hyperpolarized  $^3\text{He}$  was prepared by Rb spin-exchange<sup>9</sup> at 10 atm pressure using a 40 W laser-diode bar (Coherent Inc., Santa Clara, CA) and apparatus built by two of the authors. In the ventilation studies, approximately 0.5 l of 20–40% polarized  $^3\text{He}$  was mixed with 1–2 l nitrogen in a flexible plastic bag, and delivered to the subjects via a

mouthpiece attached to a 1 in diameter, 24 in long tube. Noseclips were applied to prevent mixing with room air. Subjects with severe emphysema were administered oxygen by nasal cannula at 2 l/min up until delivery of the  $^3\text{He-N}_2$  mixture. Although there was a limit to the maximum amount of gas that could be delivered, the volume of gas inhaled was not controlled. Rebreathing of the gas mixture from the closed system was performed for one or two cycles by three of the healthy subjects and two of those with severe emphysema. Breathing of the  $^3\text{He-N}_2$  mixture was followed by immediate washout with room air in the healthy subjects, and with the addition of oxygen delivered by nasal cannula at 2 l/s to those with severe emphysema. Imaging continued for 30–45 s after  $^3\text{He}$  inhalation. Pulse oximetry was monitored, and was not observed to fall below 85% oxygen saturation. Studies were performed with the approval of the Washington University Human Studies Committee, and informed consent was obtained from all study participants.

## RESULTS

In regions ventilated by  $^3\text{He}$ , maximum signal-to-noise ratios during the first breath ranged from approximately 20 to 40. Ventilation in the normal subjects was characterized by uniform distribution of  $^3\text{He}$  throughout most of the lungs before the end of the first breath. In the normal subject in whom each level was scanned at 0.12 s intervals, and in one of the two normal subjects scanned at 0.40 s intervals, the gas appeared first primarily in the mid-lungs, then in the lower lungs, and last in the upper lungs (Fig. 1). In one subject scanned at 0.4 s intervals, and in the two subjects scanned at 0.80 s intervals, gas seemed to appear simultaneously in all regions. Signal intensity was slightly greater in the gravitationally dependent posterior portions of the lungs. During the washout phase, no differences between lung regions in the decline of  $^3\text{He}$  signal intensity were seen. Signal intensity faded gradually and was barely detectable after two washout breaths, approximately 15–20 s after the peak of  $^3\text{He}$  inhalation.

Ventilation in patients with severe emphysema during the first breath was characterized by sequential filling of nonsegmental lung regions of variable size, with areas of absent filling interspersed (Fig. 2). Comparison of  $^3\text{He}$  and X-ray CT studies revealed no obvious focal differences in the attenuation of lung regions containing or lacking  $^3\text{He}$  signal (Fig. 2). The largest areas of absent ventilation were in the upper third of the lungs. With one rebreathing cycle (Fig. 2) and in the washout phase (Fig. 3),  $^3\text{He}$  filling of some regions not filled during the first breath occurred. Diminishment of signal during washout from  $^3\text{He}$ -containing regions was relatively uniform. Distinct areas of  $^3\text{He}$  'trapping' were not observed. The duration of signal detectability following the start of the

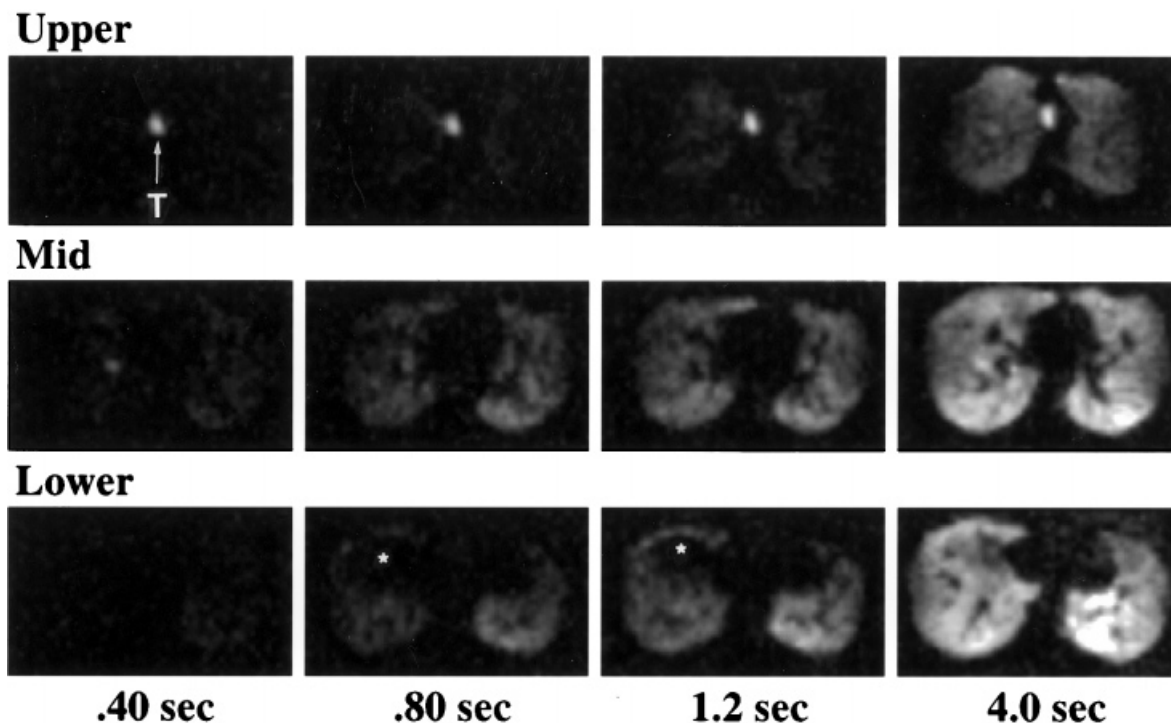


**Figure 1.** First breath  $^3\text{He}$  distribution in a normal subject. Repeated transaxial imaging at 10 levels began prior to  $^3\text{He}$  inhalation; this dynamic sequence shows three selected levels and begins with the first appearance of gas in the trachea (T). Gas appears first in the mid lung zone, then in the lower lung zone, then in the upper lung zone. Signal intensity gradually increases at each level until the end of the inhalation at 4.0 s, is slightly greater in the dependent posterior regions, and is slightly less in the upper zone compared to the mid and lower zones. The defect in anterior right lower lung (\*) at 0.80 and 1.2 s corresponds to the diaphragm and liver, which have descended below the scan plane by the end of the inhalation at 4.0 s

washout phase varied in the different patients from about 15 s to about 40 s.

## DISCUSSION

This study demonstrates that the flow and distribution of hyperpolarized  $^3\text{He}$  in the lungs during the first breath can be imaged using echo planar techniques. The two-dimensional technique used in this study requires a trade-off between temporal resolution and the number of slice locations studied. The maximum temporal resolution we could have obtained with our chosen EPI pulse sequence was 0.04 s. However, the minimum number of slice locations repeatedly scanned was three, so that ventilation in the upper, mid and lower portions of the lungs could be compared; thus, our best effective temporal resolution was 0.12 s, or 8.3 images per second at each individual level. This was sufficient to observe sequential filling at the three different slice levels in the lung during the first breath in normal subjects.

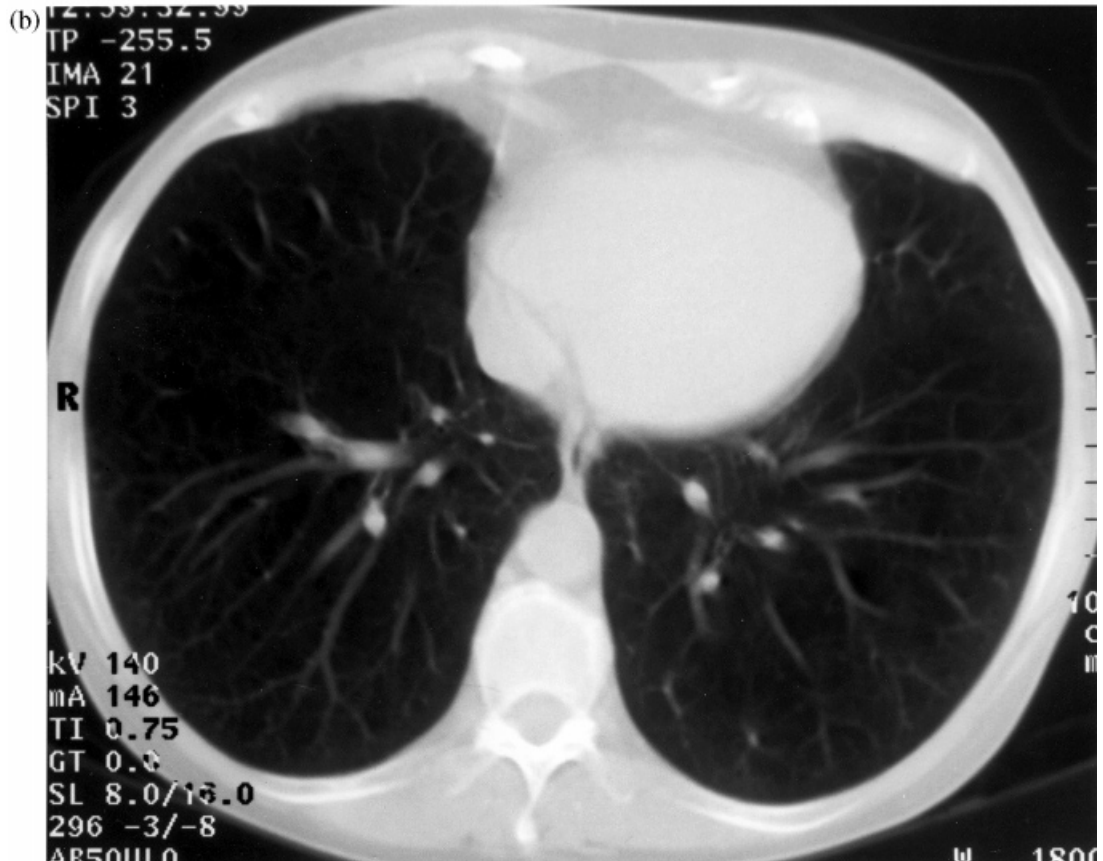
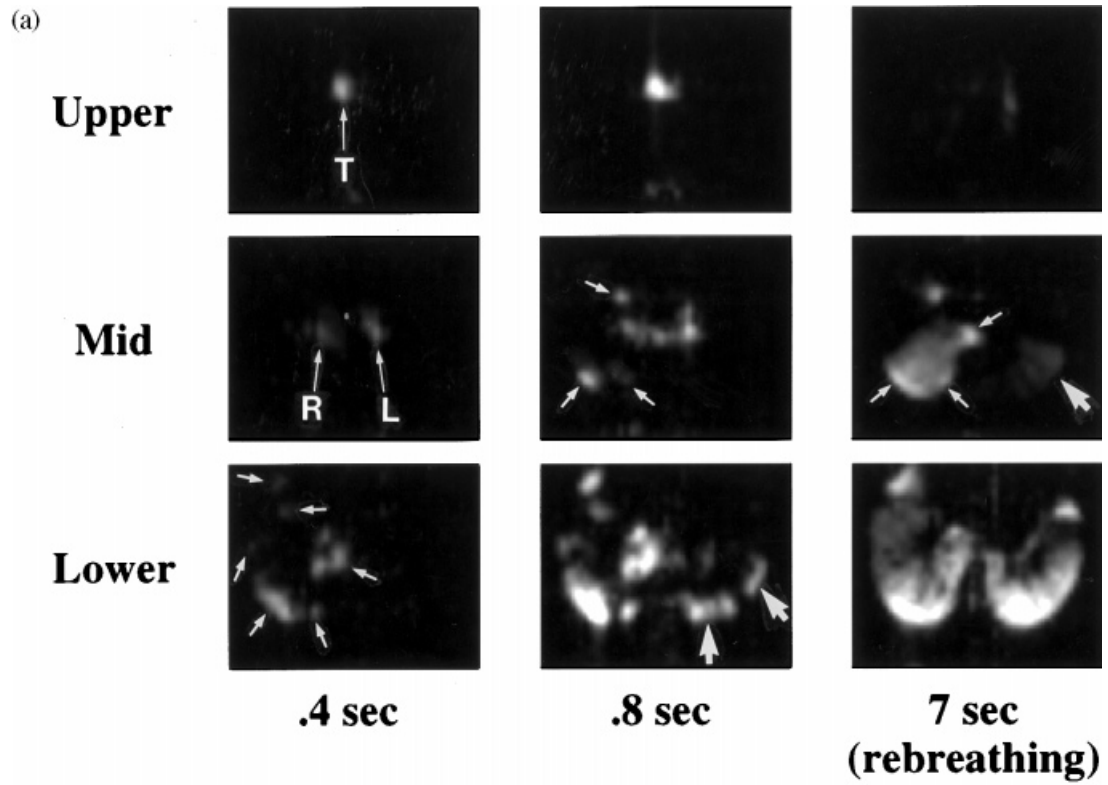
Even at this highest temporal resolution, the appearance of gas in normal subjects seemed simultaneous throughout each single slice, increasing in intensity in a relatively uniform fashion, except for slightly greater  $^3\text{He}$  density in the gravitationally dependent posterior lung

regions. As temporal resolution was decreased to 0.80 s per slice level, the ability to discriminate sequential filling at different levels decreased in the normal subjects.

In the subjects with severe emphysema, we limited temporal resolution to either 0.40 s or 0.80 s per slice level. Because lung destruction due to emphysema is nonuniform, we wanted to acquire a sufficient number of slices to adequately sample the whole lung. At this resolution, different filling rates were observed in different regions within individual slice levels. This probably reflects regional differences in compliance, airway resistance, or collateral ventilation in the diseased lung.

During rebreathing and washout with room air–nasal oxygen by patients with severe emphysema,  $^3\text{He}$  appeared in some lung regions in which it was not present at the end of the first breath inhalation. It was not possible to tell whether  $^3\text{He}$  reached these regions by antegrade flow through the airways, via the airways from adjacent lung regions (pendelluft), or by collateral pathways. However,  $^3\text{He}$  failed to appear at all during the imaging period in some regions, particularly in the upper lobes where smoking-related, centrilobular emphysema tends to be most severe.

Ventilation scintigraphy in patients with smoking related emphysema also typically shows a relative lack



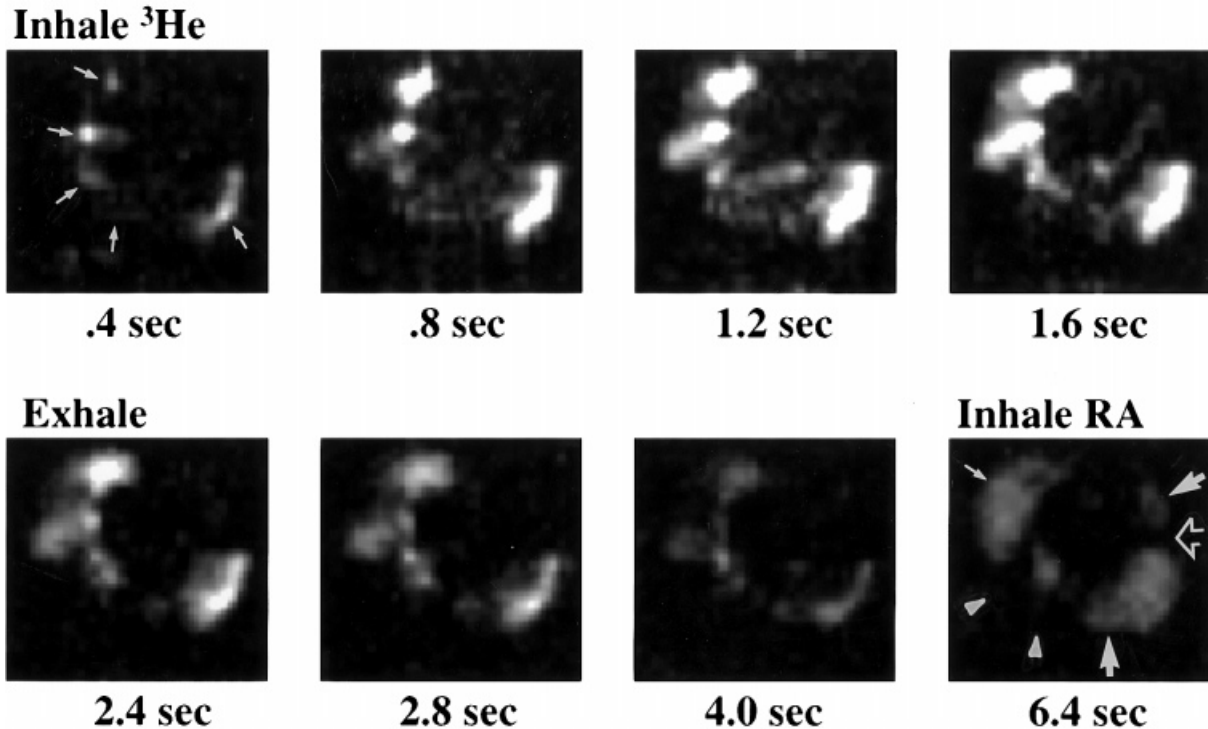


**Figure 3.** A 56-year-old woman with severe emphysema. Dynamic sequence through the mid lungs represents one of 10 transaxial levels scanned at 0.4 s intervals. The areas filled at 0.4 s (small arrows) gradually enlarge until the end of inhalation at 1.6 s, and diminish in size during exhalation from 2.4 to 4.0 s. At the end of the next inhalation of room air (which includes the  $^3\text{He}$  remaining in the airways) at 6.4 s, gas has spread to areas in the right lung (small arrow) and left lung (large arrows) not initially filled at the end of the first inhalation. A large defect persists in the right lung posteriorly (arrowheads around approximate lung margin), and a small defect persists on the left (open arrow)

of upper lobe ventilation on the first breath, but this is followed by a longer period of rebreathing during which the initially underventilated regions accumulate radioactive gas, then retain it for a prolonged period during a washout phase of several minutes. In contrast to our single-breath rebreathing of the oxygen-depleted  $^3\text{He}\text{-N}_2$  mixture, rebreathing in scintigraphic studies typically

occurs for several minutes. The short  $T_1$  of  $^3\text{He}$  polarization (approximately 34 s in the normal lung, unpublished data) therefore limits the value of the MR technique in studying the equilibrium distribution of ventilation of tracer gases. Unfortunately, our patients did not have ventilation scintigrams available for comparison.

The rapid loss of polarization also limits the ability to assess washout within the  $T_1$  decay period. The  $^3\text{He}$  polarization decays simultaneously as the gas is washing out, and this decay is enhanced by the presence of oxygen in the washout gas.<sup>10</sup> The relative contribution of each of these factors to the declining signal intensity was not distinguished.

Compared to static breath-hold techniques, images obtained with the dynamic EPI technique presented here have lower spatial resolution, and more magnetic susceptibility artifacts along the interfaces of the larger pulmonary vessels and aerated lung.<sup>8</sup> However, it is possible that  $^3\text{He}$  diffusion and collateral air flow during the breath-hold imaging period could mask ventilation defects using the static technique. A direct comparison of dynamic and static methods could determine whether either has greater sensitivity for detecting ventilation abnormalities.

**Figure 2.** A 71-year-old woman with severe emphysema. (A) Three of the 10 transaxial scan levels are shown, beginning with the first appearance of  $^3\text{He}$ . At 0.4 s, gas initially appears in several peripheral areas in the right lower lung (small arrows). At 0.8 s, the areas of filling in the right lower lung have enlarged, and gas has appeared in several small areas in the right mid lung (small arrows) and left lower lung (large arrows), although large defects persist. After two cycles of rebreathing, there is more homogeneous distribution of gas throughout both lower lungs and in the posterior right mid lung (small arrows), and the  $^3\text{He}$  signal is faintly seen in the posterior left mid lung (large arrow). During washout, the  $^3\text{He}$  signal failed to appear in the upper lungs and anterior mid lungs. T, trachea; R, right main bronchus; L, left main bronchus. (B) The X-ray CT image corresponding to the lower lung level in (A) reveals a homogeneous distribution of emphysema. No distinct regional differences are seen in the areas of ventilation defects in (A)

There are several potential clinical applications of hyperpolarized  $^3\text{He}$  MR imaging of ventilation, such as evaluation of patient suitability for lung volume reduction surgery, monitoring of lung transplant recipients for bronchiolitis obliterans syndrome,<sup>7</sup> and assessment of disease status in cystic fibrosis<sup>6</sup> and asthma. The feasibility of dynamic imaging provides an additional technique for the study of ventilation pathophysiology, disease status and response to therapy. In lung volume reduction surgery candidates, we found physiologic abnormalities involving lung regions that appeared similar to adjacent regions on X-ray CT scans. The value of this unique information in helping to select patients for lung volume reduction has yet to be assessed.

A limitation of this study is the lack of technique standardization, particularly in imaging normal lung ventilation. At the same time, this limitation suggests ways in which dynamic imaging may be used to provide new information about normal ventilation physiology, with greater temporal resolution than previously available from scintigraphic methods. Many factors that have been shown to affect the distribution of ventilation, such as posture, lung volume at the time of inhalation, the inspiratory flow rate, and the volume of gas inhaled,<sup>11</sup> were not controlled in this study. Systematic study of these factors with the temporal resolution afforded by dynamic hyperpolarized  $^3\text{He}$  MR might provide new insights. Although restriction to the horizontal position is also a limitation, the effects of position could be studied by comparing supine, prone, and decubitus positioning.

Another relative limitation is signal loss due to diffusion through the imaging gradients, which can be accentuated using EPI pulse sequences. If of sufficient magnitude, such signal loss could complicate the quantitative assessment of regional changes in signal intensity over time. However, signal loss is minimized if the voxels are of sufficient size relative to  $^3\text{He}$  diffusion rates, and can be determined quantitatively.<sup>8</sup> Assuming a diffusion coefficient of  $0.6\text{ cm}^2/\text{s}$  for  $^3\text{He}$  in areas of emphysema, we calculate that for the  $7\text{ mm}^2$  pixel dimension used in this study, diffusion through the imaging gradients results in only a 7% loss of signal. In healthy lungs, where diffusion is restricted by intact alveoli and the diffusion coefficient is smaller (approximately  $0.25\text{ cm}^2/\text{s}$ ), signal loss would be even lower.

In conclusion, dynamic  $^3\text{He}$  MR ventilation imaging

reveals the distribution of gas during a single breath, depicting normal and abnormal ventilation phenomena not seen with conventional scintigraphic methods. Imaging of equilibrium ventilation is limited using the protocol of this study, but might be improved with the use of rebreathing circuits that allow continuous oxygen delivery and carbon dioxide removal. The short  $T_1$  of hyperpolarized  $^3\text{He}$  confounds the assessment of regional gas washout; use of quantitative methods that incorporate static measurements of regional  $T_1$  decay is one potential approach to this problem. Further dynamic imaging studies may improve the understanding of ventilation in normal lungs and patients with pulmonary diseases.

## REFERENCES

1. Ebert M, Grossmann T, Heil W, Otten WE, Surkau R, Leduc M, Bachert P, Knopp MV, Schad LR, Thelen M. 1996. Nuclear magnetic resonance imaging with hyperpolarised helium-3. *Lancet* **347**: 1297–1299.
2. MacFall JR, Charles HC, Black RD, Middleton H, Swartz JC, Saam B, Driehuys B, Erickson C, Happer W, Cates GD, Johnson GA, Ravin CE. 1996. Human lung air spaces: potential for MR imaging with hyperpolarized He-3. *Radiology* **200**: 553–558.
3. Saam BT. 1996. Magnetic resonance imaging with laser-polarized noble gases. *Nat. Med.* **2**: 358–359.
4. Kauczor HU, Hofmann D, Kreitner KF, Nilgens H, Surkau R, Heil W, Potthast A, Knopp MV, Otten EW, Thelen M. 1996. Normal and abnormal pulmonary ventilation: visualization at hyperpolarized He-3 MR imaging. *Radiology* **201**: 564–568.
5. de Lange EE, Mugler JP, III, Brookeman JR, Knight-Scott J, Truweit JD, Teates CD, Daniel TM, Bogorad PL, Cates GD. 1999. Lung air spaces: MR imaging evaluation with hyperpolarized  $^3\text{He}$  gas. *Radiology* **210**: 851–857.
6. Donnelly LF, MacFall JR, McAdams HP, Majure JM, Smith J, Frush DP, Bogonad P, Charles HC, Ravin CE. 1999. Cystic fibrosis: combined hyperpolarized  $^3\text{He}$ -enhanced and conventional proton MR imaging in the lung—preliminary observations. *Radiology* **212**: 885–889.
7. McAdams HP, Palmer SM, Donnelly LF, Charles HC, Tapson VF, MacFall JR. 1999. Hyperpolarized  $^3\text{He}$ -enhanced MR imaging of lung transplant recipients: preliminary results. *American Journal of Roentgenology* **173**: 955–959.
8. Saam B, Yablonskiy DA, Gierada DS, Conradi MS. 1999. Rapid imaging of hyperpolarized gas using EPI. *Magn. Reson. Med.* **42**: 507–514.
9. Walker TG, Happer W. 1997. Spin-exchange optical pumping of noble-gas nuclei. *Rev. Mod. Phys.* **69**: 629–642.
10. Saam BT, Happer W, Middleton H. 1995. Nuclear relaxation of  $^3\text{He}$  in the presence of  $\text{O}_2$ . *Phys. Rev. A* **52**: 862–865.
11. Hughes JMB, Amis TC. Regional ventilation distribution. In: *Lung Biology in Health and Disease*, pp. 177–220. Engel LA and Paiva M, eds. New York: Marcel Dekker, (1985).